Available online at www.sciencedirect.com
SCIENCE DIRECT®
C. R. Chimie 9 (2006) 631–638
COMPTES RENDUS CHIMIE
http://france.elsevier.com/direct/CRAS2C/

Full paper / Mémoire

Modeling of photocurrent in dye-sensitized solar cells fabricated with PVDF-HFP-based gel-type polymeric solid electrolyte

Yoshinori Nishikitani *, Takaya Kubo, Tsuyoshi Asano

Central Technical Research Laboratory, Nippon Oil Corporation, 8, Chidori-cho, Naka-ku, Yokohama 231-0815, Japan

Received 22 July 2004; accepted after revision 6 January 2005

Available online 13 September 2005

Abstract

We discussed photocurrent of dye-sensitized solar cells (DSCs) with model equations of polymeric solid electrolyte (PSE)-based and liquid electrolyte-based DSCs. The short-circuit current (J_{sc}) was found out to increase even further by either increasing the diffusion coefficient of I_3^- and/or I^- or decreasing the cell-gap, or both. In particular, the cell-gap dependence of J_{sc} indicates clearly that narrowing the cell-gap is a simple, effective way to increase the J_{sc}. We also discussed the diffusion coefficient dependence of J_{sc}. The back electron transfer from TiO_2 to an oxidized dye was taken into account and explained the diffusion coefficient dependence of J_{sc} well. ***To cite this article: Y. Nishikitani et al., C. R. Chimie 9 (2006)***.

Résumé

Nous étudions la nature du photocourant généré dans des cellules solaires sensibilisées par un colorant à l'aide d'équations modélisant les cellules à électrolytes polymère solide et liquide. Le courant de court-circuit (J_{sc}) augmente d'autant plus qu'on accroît le coefficient de diffusion de I_3^- et/ou de I^- ou qu'on diminue la distance entre les électrodes. En particulier, le fait que la valeur de J_{sc} dépende de cette dernière indique clairement que le rapprochement des électrodes constitue un moyen simple et efficace d'augmenter ce courant. Nous discutons en outre de la relation entre J_{sc} et le coefficient de diffusion. Le « rétro-transfert » de l'électron de la bande de conduction du TiO_2 vers le colorant oxydé a été considéré et a permis d'expliquer pourquoi J_{sc} dépendait du coefficient de diffusion. ***Pour citer cet article : Y. Nishikitani et al., C. R. Chimie 9 (2006)***.

Keywords: Dye-sensitized solar cells; PVDF–HFP-based polymeric solid electrolyte; Photocurrent; Short-circuit current density; Back electron transfer; Diffusion coefficient of I^-–I_3^-; Smoluchowski equation

Mots clés : Cellule solaire à colorant ; Électrolyte polymère solide à base de PVDF–HFP ; Photocourant ; Densité de courant de court-circuit ; Réaction de transfert inverse ; Coefficient de diffusion du couple redox iodure–triiodure ; Équation de Smoluchowski

* Corresponding author.
E-mail address: yoshinori.nishikitani@eneos.co.jp (Y. Nishikitani).

1631-0748/$ - see front matter © 2005 Académie des sciences. Published by Elsevier SAS. All rights reserved.
doi:10.1016/j.crci.2005.02.045

1. Introduction

O'Regan and Grätzel [1] made a major breakthrough in the field of dye-sensitized photoelectrochemical cells in 1991, and opened up the possibility of practical applications as dye-sensitized solar cells (DSCs). A typical DSC comprises a nanocrystalline TiO_2 electrode sensitized with a ruthenium dye, a Pt-coated counter electrode consisting of a F-doped SnO_2 substrate, and a liquid electrolyte with a I^-/I_3^- redox couple.

DSCs are attractive for next-generation solar cells because of their potentially high conversion efficiency and the possibility of lower production cost than that of conventional silicon solar cells [2]. However, many things, such as increasing the conversion efficiency even more and achieving better durability, remain to be done before DSCs can be put on the market [3–6]. The electrolyte loss caused by the leakage and/or volatility of the electrolyte solution has been pointed out to be one of the major problem, which stays the durability of the DSC low. Various approaches to the problem have been tried before, and employing polymeric solid electrolytes (PSEs) is one of the most promising approaches. Wang et al. recently employed a PSEs containing 1-methyl-3-propylimidazolium iodide and poly(vinylidenefluoride-co-hexafluoropropylene) (PVDF-HFP) to fabricate a DSC, and a conversion efficiency of the DSC with 0.152 cm^2-active area at AM 1.5 illumination stayed at 5.3% [7].

We proposed a PVDF-HFP-based PSE film, having a good ionic conductivity and mechanical strength, for DSCs. The short-circuit current density (Jsc) of the PSE-based DSC has a strong dependence on the cell-gap, and narrower cell-gap gives a higher Jsc. We confirmed experimentally that the Jsc of a PSE-based DSC with a 20 μm cell-gap is turned out to be about 97% of a liquid electrolyte-based DSC [8].

The purpose of this paper is twofold: we discuss the photocurrent of DSCs, with model equations, focusing on the diffusion coefficient of I_3^- and/or I^-, (D_0) and the cell-gap, to find a way to achieve a higher conversion efficiency, and also explain the dependence of J_{sc} on the diffusion coefficient of I_3^- and/or I^- in terms of a back electron transfer process.

2. Experimental

The TiO_2 (Ti-nanoxide-T, Solaronix) films formed on a F-doped SnO_2 substrate (FTO: TEC15, about 15 Ω sq^{-1}, Pilkington) were 10 μm thick and 5 × 5 mm in size. The TiO_2 substrate was sensitized with a ruthenium dye (0.5 mM ruthenium-535-bis-TBA, Solaronix, in EtOH). A 30-nm-thick Pt thin film was deposited on the FTO substrate with the sputtering method, and the FTO substrate was used as a counter electrode. The liquid electrolyte was comprised of 0.5 M 1-propyl-2,3-dimethylimidazolium iodide (DMPII), 0.1 M LiI, 0.05 M I_2, 0.5 M 4-tert-butylpyridine (TBP), and one of the following solvents: methoxyacetonitril (MAN), 3-methoxypropionitril (MPN), γ-butyrolactone (GBL), and propylene carbonate (PC). The PSE film consisted of the PVDF-HFP-based matrix polymer and an electrolyte solution (0.5 M DMPII, 0.1 M LiI, 0.05 M I_2, and 0.5 M TBP in GBL). The electrolyte content of the PSE film was determined from $(m_0–m_d)/m_0$; m_0 and m_d are the weight of an as-formed PSE film and a dry, solvent-free PSE film, respectively.

The diffusion coefficient of I_3^- and/or I^- in electrolytes were evaluated using the Cottrell equation [9], $i(t) = n\,F\,A\,D_0^{1/2}\,C_0(\text{init})/\pi^{1/2}\,t^{1/2}$, where $n = 2$, F is the Faraday constant, and C_0(init) is the initial concentration of I_3^-. The current–voltage characteristic was measured with a potentiostat (1287 Solartron) under illumination (AM1.5, 100 mW cm^{-2}, surface temperature of the DSC at 27 °C) using solar simulator (YSS-150, Yamashita-Denso) equipped with a cooling stage. The current–voltage curves were measured by using cyclic voltammetry at 10 mV s^{-1}. The cell-gap is defined here as the distance between the surfaces of the FTO and Pt layer. We selected a cell-gap by changing the thickness of either the PSE or spacer film in the case of a liquid electrolyte.

3. Results and discussion

3.1. Dependence of photocurrent on diffusion coefficient of I_3^- and/or I^-

The DSC goes through the series of reactions to complete power generation. These reactions are the electron injection from a photo-excited dye to TiO_2, the electron conduction in TiO_2, reduction of I_3^- to I^- at a counter electrode, and the diffusion of I^- to TiO_2, and the reduction of an oxidized dye to a neutral dye there. In theory, the maximum conversion efficiency of a DSC depends solely on an absorption spectrum of a dye used

(referred to as photon-limiting case hereafter). In practice, however, part of the electron injected to TiO_2 annihilates due to a back electron transfer to I_3^- and an oxidized dye. Therefore, the sunlight absorption of the dye hardly becomes a rate limiting process in power generation of a solar cell, but the ionic conduction of I^- and/or I_3^- in an electrolyte does, for example.

We then derive model equations for J_{sc} of DSCs as a function of a cell-gap and I_3^- diffusion coefficient, and discuss their effects on the performance of DCSs. To do so, the model equations given by Papageorgiou et al. [10] are extended so that we are able to discuss not only liquid electrolyte-based DSCs but also PSE-based DSCs. For simplicity, in modifying the model equations, we assumed the diffusion coefficient of I_3^- in a PSE to relate with that in a liquid electrolyte through the form of $D = \alpha\, D_0$, where D and D_0 are diffusion coefficients, respectively, of a PSE and a liquid electrolyte, and α a liquid electrolyte content in the PSE. The symbols used to describe the equations are given in Fig. 1, and summarized in Table 1 for the sake of clarity.

When the photon-limiting current flows, the concentration profiles of I_3^- in a TiO_2 nanopore region (Region I: $0 < x \le \ell$) and in a bulk electrolyte region (Region II: $\ell < x < \ell + b$) are given below; ℓ is a TiO_2 film thickness and b is a bulk electrolyte layer thickness.

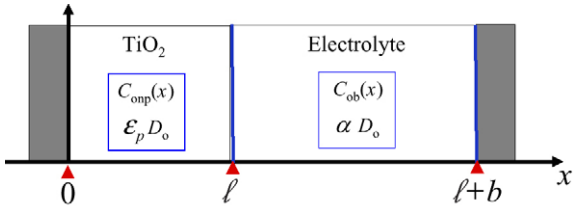

Fig. 1. Schematic cross-sectional view of DSC.

Table 1
List of symbols given in Fig. 1

$C_{ob}(x)$	Triiodide concentration in electrolyte at position x
$C_{onp}(x)$	Triiodide concentration in TiO_2
C_0(init)	Initial concentration of triiodide
J_{lim}	Short-circuit current density (lim: diffusion-limiting case)
D_0	Diffusion coefficient of triiode
ε_p	Porosity of TiO_2
α	Liquid electrolyte (LE) content in PSE
ℓ	TiO_2 film thickness
b	Electrolyte layer thickness

Region I: $0 < x \leqslant \ell$

$$C_{onp}(x) = C_0(\text{init}) + \frac{J_{ph}\,\ell}{D_0\,F\,\varepsilon_p}\left[\begin{array}{l} -\dfrac{1}{6\,f_{PE}\left(1+\dfrac{\alpha\,b}{\varepsilon_p\,\ell}\right)} + \dfrac{\left(\dfrac{b}{\ell}\right)^2}{4\left(1+\dfrac{\alpha\,b}{\varepsilon_p\,\ell}\right)} - \dfrac{1}{2\,A_\lambda\,\ln(10)} \\ +\dfrac{10^{A_\lambda}}{2(10^{A_\lambda}-1)} - \dfrac{10^{A_\lambda}}{2(10^{A_\lambda}-1)}\left\{\dfrac{x}{\ell} - \dfrac{1}{A_\lambda\,\ln(10)}\left(1-10^{-A_\lambda\frac{x}{\ell}}\right)\right\} \end{array}\right] \tag{1}$$

Region II: $\ell < X \le \ell + b$

$$C_{ob}(x) = C_0(\text{init}) + \frac{J_{ph}\,\ell}{D\,F\varepsilon_p}\left[-\frac{1}{6\,f_{PE}\left(1+\dfrac{\alpha\,b}{\varepsilon_p\,\ell}\right)} + \frac{\left(\dfrac{b}{\ell}\right)^2}{4\left(1+\dfrac{\alpha\,b}{\varepsilon_p\,\ell}\right)} - \frac{\varepsilon_p\,(x-\ell)}{2\,\alpha\,\ell}\right] \tag{2}$$

$$f_{PE}(A_\lambda) = \frac{2}{3}\,\frac{A_\lambda^2\left\{\ln(10)\right\}^2(10^{A_\lambda}-1)}{A_\lambda^2\left\{\ln(10)\right\}^2 10^{A_\lambda} + 2\,A_\lambda\,\ln(10) - 2\,(10^{A_\lambda}-1)} \tag{3}$$

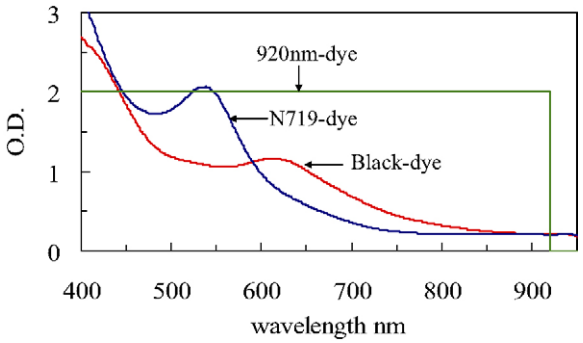

Fig. 2. Absorption spectra of three different dyes used for DSC. The maximum or photon-limiting photocurrent supposed to be achieved in case of the photon-limiting case for N-719, Black-dye, and 920 nm-dye are 16, 20.5, and 28 mA cm^{-2}, respectively.

$C_{onp}(x)$ and $C_{ob}(x)$ are I_3^- concentrations at a position of x, respectively, in a TiO_2 nanopore electrolyte and in a bulk electrolyte, and C_0(init) an initial concentration of I_3^-. ε_p is a porosity of TiO_2. The equations become the ones given by Papageorgiou et al. [10] in the case of a liquid electrolyte, i.e. $\alpha = 1$.

We calculated the concentration profiles of I_3^- in the DSCs, employing three different sensitizing-dyes and two different cell-gaps. The two of the dyes are commonly used ones in DSCs, cis–bis(isothiocyanato)bis(2,2′-bipyridyl-4,4′-dicarboxylato)- ruthenium(II) bis-tetrabutylammonium (N719) and tris(isothiocyanato)-ruthenium(II)-2,2′:6′,2″-terpyridine-4,4′,4″-tricarboxylic acid, tris-tetrabutylammonium salt (black dye), and the third one is a hypothetical dye(920 nm-dye) with a sharp absorption edge at 920 nm, i.e. the optimal threshold for single junction solar cells [2]. The absorption spectra of the three dyes are given in Fig. 2. The maximum or photon-limiting photocurrent supposed to be achieved in the case of the photon-limiting for N-719, Black-dye, and 920 nm-dye are 16, 20.5, and 28 mA cm^{-2}, respectively [2]. The I_3^- concentration profiles between the electrodes are shown in Fig. 3. The concentration profiles of I_3^- in DSCs with 50 μm cell-gap indicate that J_{sc}s flow under diffusion-limiting conditions in all the cases since the concentration of I_3^- at the Pt-counter electrode ($x = 50$ μm) can not be greater than zero as shown in Fig. 3. In contrast, the photocurrent of the DSCs with the cell-gap of 20 μm flows under photon-limiting conditions except for the PSE-based DSC formed with 920 nm dye.

We now focus our attention on the minimum diffusion coefficient required to obtain the photon-limiting photocurrent. The photocurrent flowing under diffusion-limiting conditions is given in Eq. (4).

$$J_{lim} = \frac{6\varepsilon_p F D_0 C_0(\text{init})}{\ell} \frac{1 + \dfrac{\alpha b}{\varepsilon_p \ell}}{\dfrac{1}{f_{PE}} + 3\dfrac{\varepsilon_p b}{\alpha \ell} + \dfrac{3}{2}\left(\dfrac{b}{\ell}\right)^2} \quad (4)$$

The minimum diffusion coefficients for the DSCs, tabulated in Table 2, are estimated by equating J_{lim} to J_{ph}. The diffusion coefficient I_3^- and/or I^- of the DSC

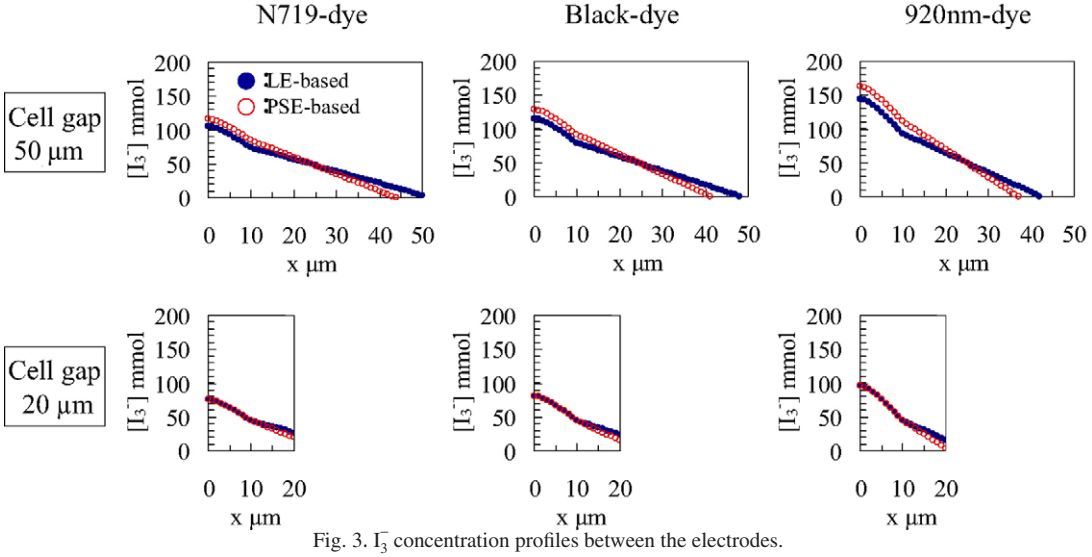

Fig. 3. I_3^- concentration profiles between the electrodes.

Table 2
Minimum diffusion coefficient of I_3^- obtained on 12 different DSCs

Cell gap μm	$D_{min} \times 10^{-6}$ cm^2 s^{-1}					
	N719 (I_{ph} = 16 mA cm^{-2})		Black-dye (I_{ph} = 20.5 mA cm^{-2})		92 nm-dye (I_{ph} = 28 mA cm^{-2})	
	solution	PSE	solution	PSE	solution	PSE
50	4.4	6.4	5.6	8.2	7.6	11.2
20	1.8	2.6	2.3	3.4	3.2	4.6

with a 50 μm cell-gap is required to be twice as high as the corresponding value of the 20 μm cell-gap DSC. Therefore, the cell-gap dependence shows clearly that narrowing the cell-gap is a simple, effective way to increase the J_{sc}.

3.2. Equivalent circuit analysis of photocurrent in DSCs

In this section, the short-circuit current density of DSCs are discussed in terms of diffusion coefficients of I_3^- and/or I^-. Fig. 4 shows the current density–voltage (J–V) curves for DSCs with four different electrolyte solvents; MAN, MPN, GBL, and PC. As shown in Fig. 4, one of the characteristic features of the *J–V* curves is that the entire shape of a *J–V* curve is similar to each other irrespective of diffusion coefficients, but J_{sc} values decrease with decreasing the diffusion coefficient of I_3^- and/or I^-. The *J–V* characteristics of DSCs have been often discussed with an equivalent circuit depicted schematically in Fig. 5 by analogy with conventional p–n junction solar cells. The equation for the equivalent circuit is given by Eq. (5) [11].

$$J = J_{ph} - J_0\left[\exp\left\{\frac{q(V + R_s J)}{nkT}\right\} - 1\right] - \frac{V + R_s J}{R_{sh}} \quad (5)$$

Here J_0 is the saturation current density, R_s the series resistance, R_{sh} the shunt resistance, q the electric charge, n the ideality factor, k the Boltzman constant, and T the temperature. J_0 is mainly determined by the back electron transfer process from TiO_2 to I_3^-, and the R_s is composed chiefly of the resistance of a FTO thin film and a nanoporous TiO_2 film, and ionic resistance of an electrolyte layer. The R_s is then given by Eq. (6) since the resistance of the electrolyte is assumed to change inversely proportional to the diffusion coefficient of I_3^- and/or I^- in the electrolyte.

$$R_s = R_0 + R_1 = R_0 + \frac{a}{D} \quad (6)$$

In Fig. 6, the series resistance values of DSCs with four different electrolyte solvents are plotted with the reciprocal value of diffusion coefficient of I_3^- and/or I^-. Series resistance values were obtained from AC imped-

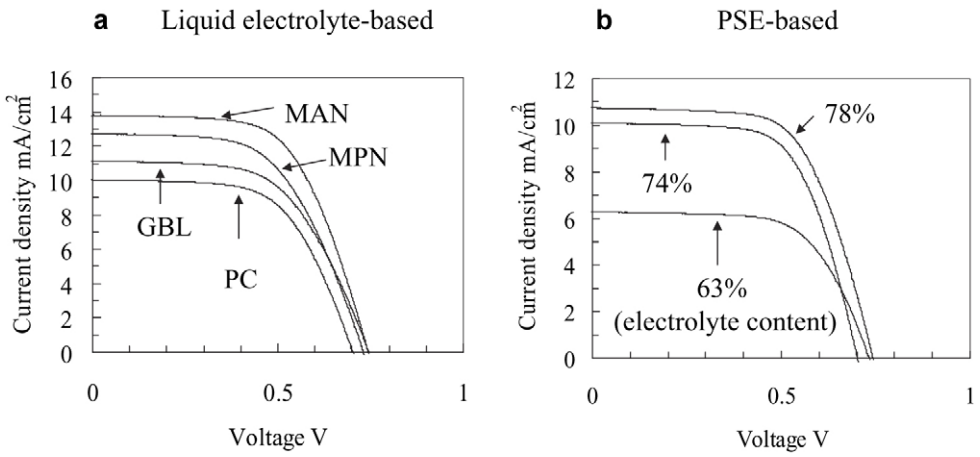

Fig. 4. Current–voltage curves of liquid-electrolyte-based and PSE-based DSCs.
MAN; methoxyacetonitril, MPN; 3-methoxypropionitril, GBL; γ-butyrolactone, and PC; propylene carbonate.

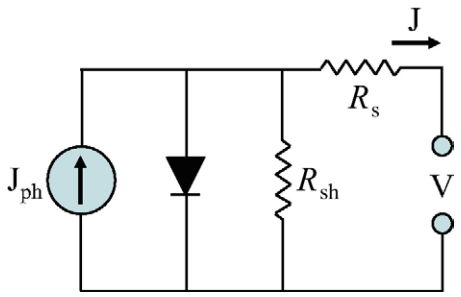

Fig. 5. Equivalent circuit for DSC. R_s; series resistance, R_{sh}; shunt resistance.

ance spectra [8]. The experimental data (solid-squares) was fitted well with Eq. (6) (solid-line). The slope and the intercept at the axis of ordinate of the straight line give a and R_0, respectively. Under short-circuit conditions, the relationship between the diffusion coefficients of I_3^- and/or I^- and short-circuit current density was derived into the form of Eq. (7): the third-term of Eq. (5) is neglected because R_{sh} is quite large.

$$D = a\,\frac{q\,J_{sc}}{n\,k\,T}\left\{\frac{1}{\ln\left(\dfrac{J_{ph}+J_0-J_{sc}}{J_0}\right)-\dfrac{qR_0\,J_{sc}}{nkT}}\right\} \quad (7)$$

V_{oc} and J_{sc} are obtained from the *J–V* curves measured with various irradiation intensities. V_{oc} values plotted with their respective J_{sc} on a semi-logarithm scale gives a straight line as shown in Fig. 7, from the slope of which the ideality factor was obtained to be about 1.8 for all the DSCs. Fig. 8 gives the J_{sc} dependence on the diffusion coefficient in liquid electrolyte-based DSCs and PSE-based DSCs. We fitted the experimental data with Eq. (7) using the known ideality factor of 1.8. The best-fitted curve shown as a solid-line in Fig. 8 was obtained when the J_0 was adjusted to 1.06×10^{-4} A cm^{-2}. This J_0 value is five to six orders of magnitude larger than given in previous literatures [12–14]. A typical J_0 value is in a range from 10^{-9} to 10^{-8} A cm^{-2}, which was, however, confirmed to reproduce the experimental data with Eq. (7) far from satisfactory. We have been employing the fixed J_{ph} of 16 mA cm^{-2} all the way through the discussion. In practice, the J_{ph} value is found out to depend on the diffusion coefficient. Actually a similar J_{ph} dependence on the ionic conductivity, or equivalently the diffusion coefficient, of polyacrylate derivative PSEs has been reported by Yanagida et al. [14]. We then focus on the

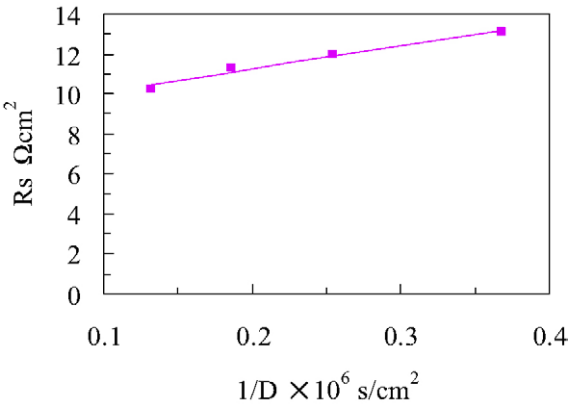

Fig. 6. Series resistance values of DSCs with four different electrolyte solvents are plotted with the reciprocal value of diffusion coefficient of I_3^- and/or I^-.

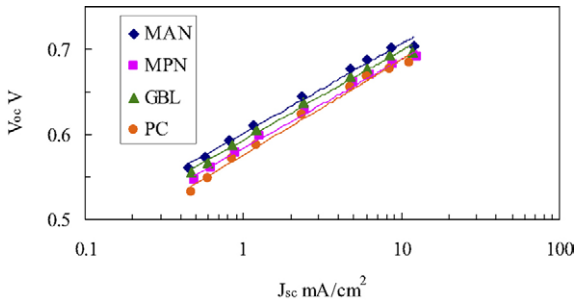

Fig. 7. Relation between short-circuit current density and open circuit voltage.
MAN; methoxyacetonitril, MPN; 3-methoxypropionitril, GBL; γ-butyrolactone, and PC; propylene carbonate.

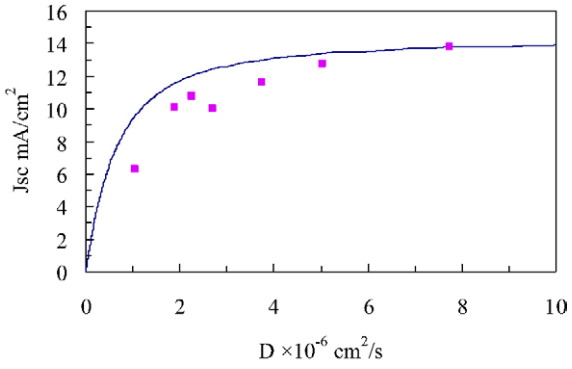

Fig. 8. Short-circuit current density dependence on diffusion coefficient of liquid electrolyte-based and PSE-based DSCs. Experimental data; square, best-fitted curve; solid line. $J_{ph} = 16 \times 10^{-3}$ A cm^{-2}, n = 1.80, $R_0 = 8.93$ Ω cm^{-2} $q = 1.6 \times 10^{-19}$ C, $k\,T = 4.11 \times 10^{-21}$ J, $a = 1.16 \times 10^{-5}$ Ω cm^4 s^{-1}. $J_0 = 1.06 \times 10^{-4}$ A cm^{-2}; this value is about three orders of magnitude greater than typical values reported in previous literatures.

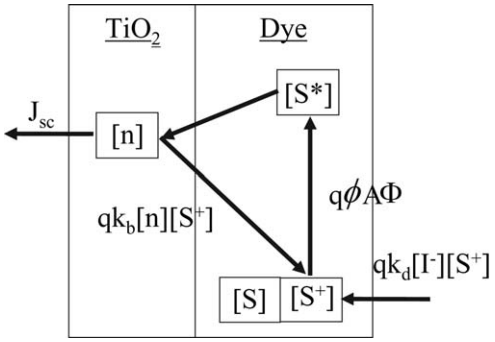

Fig. 9. Schematic diagram of operating principle of DSC. k_b and k_d are the rate constants, respectively, for back and forward electron transfer reactions, [n] the electron density in TiO_2, [S^+] the oxidized dye concentration, ϕ the electron injection efficiency, Φ the incident photon flux, and A the ratio of absorbed photon flux to Φ.

back electron transfer from the nanoporous TiO_2 to an oxidized dye, besides the back electron transfer to I_3^-. This process is usually neglected because the reduction of the oxidized dye by I^- is assumed to take place well before an electron in TiO_2 reduces the oxidized dye. It is, however, pointed out that this process becomes not negligible in the case of a DSC with an electrolyte of low I_3^- diffusion coefficient [12]. This is because I^- may not diffuse in nanoporous TiO_2 freely and part of oxidized dyes remains unchanged as it is without being reduced by I^-.

A schematic diagram of the operating principle of a DSC under short-circuit conditions is given in Fig. 9. The operation process is composed of the following fundamental steps.

Forward electron transfer process:

- the dye absorbs the sunlight and an electron is photoexcited from a ground state to an excited state;
- the electron is injected from the excited dye to a TiO_2 conduction band, leaving behind an oxidized dye;
- the electron is extracted through the TiO_2 conduction band;
- the oxidized dye is reduced by I^-, returning back to its initial neutral state.

Backward electron transfer process:

- part of the injected electrons in the TiO_2 recombines with the oxidized dye.

Here, k_b and k_d are the rate constants, respectively, for back and forward electron transfer reactions, [n]: electron density in TiO_2, [S^+]: the oxidized dye concentration, ϕ: electron injection efficiency, Φ: incident photon flux, and A: the ratio of absorbed photon flux to Φ.

The series of equations for photo- and electrochemical kinetics in a DSC operating under steady state conditions is given below.

$$\frac{d[S^+]}{dt} = \phi\, A\, \Phi - k_b\,[n][S^+] - k_d\,[I^-][S^+] = 0 \tag{8}$$

$$\ell\,(1-\varepsilon_p)\,\frac{d[n]}{dt} = \phi\, A\, \Phi - k_b\,[n][S^+] - k_d\,[I^-][S^+] = 0 \tag{9}$$

$$J_{sc} = q k_d [I^-][S^+] \tag{10}$$

The electron concentration in the nanoporous TiO_2 at a steady state equals summation of the initial concentration of electrons, [n_0], at $t = 0$ and the concentration of steadily injected electrons from the excited dye. The balance equation is then

$$\ell(1-\varepsilon_p)[n] = \ell(1-\varepsilon_p)[n_0] + [S^+] \tag{11}$$

where ℓ is the thickness of the TiO_2 layer.

The short-circuit current density is derived from Eqs. (8)–(11) in the following form;

$$J_{sc} = \frac{q\,k_d\,[I^-]\left\{-(k_b[n_0] + k_d[I^-]) + \sqrt{(k_b[n_0] + k_d[I^-])^2 + \dfrac{4\,k_b\,\phi\,A\,\Phi}{\ell(1-\varepsilon_p)}}\right\}}{\dfrac{2\,k_b}{\ell(1-\varepsilon_p)}} \tag{12}$$

The equation is approximated to be

$$J_{sc} = \frac{k_d\,[I^-]}{k_b\,[n_0] + k_d\,[I^-]} q\phi A\Phi = \frac{k_d\,[I^-]}{k_b\,[n_0] + k_d\,[I^-]} J_{ph} \tag{13}$$

because $(k_b\,[n_0] + k_d\,[I^-])^2 > 4\;k_b\,\phi\,A\,\Phi/\,l(1-\varepsilon_p)$.

The Smoluchowski equation gives the relationship between k_d and D, that is, $k_d = \gamma\, D\, \lambda$ [15]. Although γ was originally assigned to 4 π, γ given in the equation

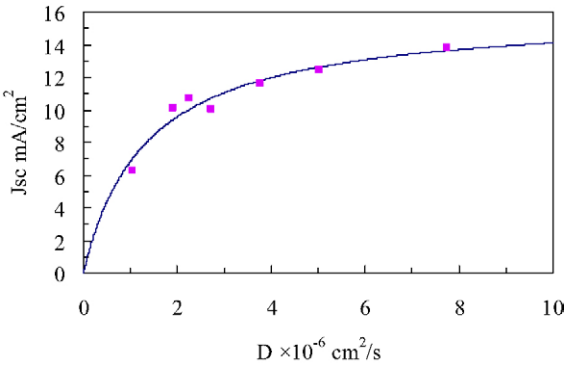

Fig. 10. Short-circuit current density dependence on diffusion coefficient of liquid electrolyte-based and PSE-based DSCs. Experimental data; square, best-fitted curve; solid-line $J_{ph} = 16 \times 10^{-3}$ A cm^{-2}, $\lambda = 5.13 \times 10^{-8}$ cm, $[I^-] = 5.5 \times 10^{-4}$ cm^{-3} $k_b = 2.74 \times 10^{-12}$ s^{-1}, $[n_0] = 1.96 \times 10^{17}$ cm^{-3}, $\gamma = 2.35 \times 10^{-2}$.

is a constant value less than 4 π because I^- can only approach to S^+ from a limited solid angle. With the Smoluchowski equation, J_{sc} is rewritten as a function of D:

$$J_{sc} = \frac{\gamma\ D\ \lambda[I^-]}{k_b\ [n_0] + \gamma\ D\ \lambda\ [I^-]} J_{ph} \tag{14}$$

The experimental data shown in Fig. 10 were fitted well with Eq. (14) by least-squares method. The fitting parameters thus obtained are as follows: $[n_0] = 1.96 \times 10^{17}$ cm^{-3}, $\gamma = 2.35 \times 10^{-2}$, $\lambda = 5.13 \times 10^{-8}$ cm, $k_b = 2.74 \times 10^{-12}$ s^{-1}. The first term on the right side of Eq. (5) becomes a leading term under short-circuit conditions because $V = 0$, and J_{ph} in Eq. (5) should be replaced by Eq. (15) then;

$$J = \frac{\gamma\ D\ \lambda[I^-]}{k_b\ [n_0] + \gamma\ D\ \lambda\ [I^-]} J_{ph} - J_0 \left[\exp\left\{ \frac{q\ (V + R_s\ J)}{nkT} \right\} - 1 \right] - \frac{V + R_s\ J}{R_{sh}} \tag{15}$$

It is concluded that a back electron transfer from TiO_2 to an oxidized dye also appear to influence on J_{sc} particularly when diffusion coefficient of I_3^- and/or I^- is low enough for an oxidized dye to be reduced before the back electron transfer reaction occurs [12].

The electron injection efficiency and incident photon flux are assumed to be constant all the way through the discussion because the electrolyte compositions used are essentially same in all the samples except for the matrix polymer and solvent.

4. Conclusion

We discussed photocurrent of DSCs with model equations of the two types of DSCs, choosing three different sensitizing-dyes; N719-, black-, and 920 nm-dyes. The J_{sc} is found out to increase even further by either increasing the diffusion coefficient of I_3^- or decreasing the cell-gap, i.e. ℓ, or both. In particular, the cell-gap dependence indicates clearly that narrowing the cell-gap is a simple, effective way to increase the J_{sc}. The J_{sc} J_{sc}'s of the DSCs studied here reach quite close to the J_{ph}, if the cell-gap is reduced to 20 μm. The J–V characteristics of the DSCs were discussed by analogy with conventional p–n junction solar cells. We also discussed the diffusion coefficient dependence of J_{sc}. The back electron transfer from TiO_2 to an oxidized dye was taken into account, which explained the diffusion coefficient dependence of J_{sc} well.

References

[1] B. O'Regan, M. Grätzel, Nature 353 (24) (1991) 737.
[2] M. Grätzel, J. Photochem. Photobiol. C 4 (2003) 145.
[3] A. Hagfeldt, M. Grätzel, Acc. Chem. Res. 33 (2000) 269.
[4] K. Hara, M. Kurashige, S. Ito, A. Shinpo, S. Suga, K. Sayama, H. Arakawa, Chem. Commun. (2003) 252.
[5] H. Lindström, A. Holmberg, E. Magnusson, S.-E. Lindquist, L. Malmqvist, A. Hagfeldt, Nano Lett. 1 (2001) 97.
[6] T. Miyasaka, Y. Kijitori, T.N. Murakami, M. Kimura, S. Uegusa, Chem. Lett. (Jpn) (2002) 1250.
[7] P. Wang, S.M. Zakeeruddin, I. Exnar, M. Grätzel, Chem. Commun. (2002) 2972.
[8] T. Asano, T. Kubo, Y. Nishikitani, J. Photochem. Photobiol. A: Chem. 164 (2004) 111.
[9] A.J. Bard, L.R. Faulkner, in: Electrochemical Methods; Fundamentals and Applications, 2nd ed, John Wiley & Sons, New York, 2001, p. 163.
[10] N. Papageorgiou, M. Grätzel, P.P. Infelta, Sol. Energy Mater. Sol. Cells 44 (1996) 405.
[11] S.M. Sze, in: Physics of Semiconductor Devices, 2nd ed, John Wiley & Sons, New York, 1981, p. 806.
[12] M. Yanagida, T. Yamaguchi, M. Kurashige, K. Hara, R. Katoh, H. Sugihara, H. Arakawa, Inorg. Chem. 42 (2003) 7921.
[13] S. Södergren, A. Hagfeldt, J. Olsson, S.-E. Lindquist, J. Phys. Chem. 98 (1994) 5552.
[14] M. Matsumoto, Y. Wada, T. Kitamura, K. Shigaki, T. Inoue, M. Ikeda, S. Yanagida, Bull. Chem. Soc. Jpn 74 (2001) 387.
[15] M. Smoluchowski, Z, Phys. Chem. 92 (1917) 129.